

Collision Dynamics of Polarized Solitons in Linearly Coupled Nonlinear Schrödinger Equations

Michail D. Todorov* and Christo I. Christov†

**Department of Differential Equations, Faculty of Applied Mathematics and Informatics
Technical University of Sofia, 1000 Sofia, Bulgaria*

*†Department of Mathematics, University of Louisiana at Lafayette
Louisiana, 70504-1010 LA, USA*

Abstract. The system of linearly coupled nonlinear Schrödinger equations is solved by a conservative difference scheme in complex arithmetic. The initial condition represents a superposition of two one-soliton solutions of linear polarizations. The head-on and takeover interaction of the solitons and their quasi-particle (QP) behavior is examined in conditions of rotational polarization and gain. We found that the polarization angle of a quasi-particle can change independently of the collision.

Keywords: Linearly coupled nonlinear Schrödinger equations, rotational polarization, breathing solitons

PACS: 07.05.Tp, 42.25.Ja, 94.05.Fg, 94.05.Pt

INTRODUCTION

Investigating the soliton dynamics in both linearly and nonlinearly Coupled Nonlinear Schrödinger Equations (CNLSEs) is of great importance from several different perspectives. The main ones are the propagation of optical pulses in optical fibers [1, 5] and the investigation of the quasi-particle (QP) behavior of soliton solutions. The essential new feature of CNLSEs in comparison with the single NLSE is the polarization, which is related to relative amplitudes of the components. Keeping in mind the fact that each component is actually a complex-valued function, one can appreciate the complexity of the possible soliton interactions. The role of the nonlinearity in the interaction of initially linearly and elliptically polarized solitons was investigated in [8, 10]. It was uncovered that depending on the magnitude of the cross-modulation parameter (presenting the nonlinear coupling), the interaction between the modes during the collision, changes the polarization of the QPs, and/or gives birth to one or more QPs. On the other hand, the CNLSEs model has richer phenomenology when a linear coupling is considered alongside with the main, nonlinear coupling (see, e.g., [7] and the literature cited therein). This quantity generates rotational polarization which is independent of initial polarization of the soliton system. This is the reason to focus our attention to the dynamics of the soliton solutions in the Manakov system when a linear coupling is present.

PROBLEM FORMULATION

Let us consider a linearly coupled system of nonlinear Schrödinger equations (LC-NLSEs)

$$i\psi_t = \beta \psi_{xx} + \alpha_1 (|\psi|^2 + |\phi|^2) \psi + \Gamma \phi, \quad (1a)$$

$$i\phi_t = \beta \phi_{xx} + \alpha_1 (|\phi|^2 + |\psi|^2) \phi + \Gamma \psi, \quad (1b)$$

where β is the dispersion coefficient, α_1 parameterizes the self-focusing in birefringent media. This system possesses three conservation laws when asymptotic boundary conditions are imposed, namely when $\psi, \phi \rightarrow 0$ for $x \rightarrow \pm\infty$. Following [3, 7] we define “mass”, M , (pseudo)momentum, P , and energy, E as follows

$$M \stackrel{\text{def}}{=} \frac{1}{2\beta} \int_{-L_1}^{L_2} (|\psi|^2 + |\phi|^2) dx, \quad P \stackrel{\text{def}}{=} - \int_{-L_1}^{L_2} \mathcal{I}(\psi \bar{\psi}_x + \phi \bar{\phi}_x) dx, \quad E \stackrel{\text{def}}{=} \int_{-L_1}^{L_2} \mathcal{H} dx, \quad (2)$$

where

$$\mathcal{H} \stackrel{\text{def}}{=} \beta (|\psi_x|^2 + |\phi_x|^2) - \frac{\alpha_1}{2} (|\psi|^2 + |\phi|^2)^2 + 2\Gamma [\Re(\bar{\psi}\phi)]$$

is the Hamiltonian density of the system. Here $-L_1$ and L_2 are the left end and the right end of the interval under consideration. The following conservation/balance laws hold, namely

$$\frac{dM}{dt} = 0, \quad \frac{dP}{dt} = \mathcal{H}|_{x=L_2} - \mathcal{H}|_{x=-L_1}, \quad \frac{dE}{dt} = 0, \quad (3)$$

which means that for asymptotic boundary conditions LCNLSEs admit at least three conservation laws. Unfortunately there is no indication in the literature that the system (1a)-(1b) admits more conservation laws or that it is fully integrable.

The system under consideration is of Manakov type with additional linear coupling that leads to oscillation of the maximal height of the localized pulses (‘breathing’) even when they are not noninteracting. This can be shown analytically following [7] through the substitution

$$\psi = \Psi \cos(\Gamma t) + i\Phi \sin(\Gamma t), \quad (4a)$$

$$\phi = \Phi \cos(\Gamma t) + i\Psi \sin(\Gamma t), \quad (4b)$$

which reduces the original linearly coupled system Eqs. (1) to the ubiquitous Manakov system for functions Ψ and Φ . In order to create a numerical tool that allows expansion to more complicated cases, we will solve the original system (1) rather than the reduced system for Ψ and Φ .

The linear coupling parameter Γ can be, in general, a complex number. The real part $\Gamma_r = \Re[\Gamma]$ governs the oscillations between states termed as breathing solitons, while the imaginary part $\Gamma_i = \Im[\Gamma]$ is responsible for the the gain/dissipation behavior of soliton solutions. Eqs. (1) possess solutions, which are combinations of interacting solitons oscillating with frequency Γ_r . These solutions are pulses whose modulation amplitude is of general form (non-*sech*) and their polarization rotates with time. This determines

the choice of initial conditions for numerical investigation of temporal evolution of interacting solitons.

The soliton solutions (QPs) are localized envelopes on a propagating carrier wave. For streamlining the notation, it is convenient to introduce the vectors $\vec{\chi} = (\psi, \phi)^T$ and $\vec{\delta} = (\delta_\psi, \delta_\phi)^T$. Then the initial condition is constructed as the superposition of two QPs situated at X_l and X_r , and propagating with phase speeds c_l and c_r , i.e.,

$$\vec{\chi}(x, 0) = \vec{\chi}_l(x, 0, c_l, n_l, X_l, \vec{\delta}_l) + \vec{\chi}_r(x, 0, c_r, n_r, X_r, \vec{\delta}_r). \quad (5)$$

Here $|X_r - X_l|$ has to be large enough so the ‘tail’ of the first QP is fairly well decayed at the position of the second QP. In this paper the scalar form of each QP in right-hand side of (5) is assumed to be *sech*-like, i.e.,

$$(\psi, \phi)^T(x, t; X, c, n) = (A_\psi, A_\phi)^T \text{sech}[b(x - X - ct)] \exp \left\{ i \left[\frac{c}{2\beta} x + nt + \delta_{\psi, \phi} \right] \right\} \quad (6)$$

where n is the carrier frequency; $\delta_{\psi, \phi}$ are the phases of the two components. Note that the phase speed is the same for the two components ψ and ϕ . If they propagate with different phase speeds, the two components will be in two different positions in space after some time, no longer forming a single structure.

NUMERICAL METHOD

In order to obtain reliable results for the time evolution of the solution, one needs a difference scheme that represents faithfully the above mentioned conservation laws. Such a scheme was proposed in [3], and applied in [7]. This scheme was based on a fast Gaussian elimination solver for multi-diagonal systems. Consequently, this scheme was implemented for complex arithmetic in [8] using a solver generalizing [4] to the case of complex-valued multi-diagonal systems. The complex-arithmetic algorithm is four times faster, and we use it also in the present paper. Thus, for solving Eqs. (1a)-(1b) with the initial conditions (4a)-(4b) numerically, we use an implicit conservative scheme in complex arithmetic:

$$i \frac{\psi_i^{n+1} - \psi_i^n}{\tau} = \frac{\beta}{2h^2} (\psi_{i-1}^{n+1} - 2\psi_i^{n+1} + \psi_{i+1}^{n+1} + \psi_{i-1}^n - 2\psi_i^n + \psi_{i+1}^n) \\ + \alpha_1 \frac{\psi_i^{n+1} + \psi_i^n}{4} \left[(|\psi_i^{n+1}|^2 + |\psi_i^n|^2) + (|\phi_i^{n+1}|^2 + |\phi_i^n|^2) \right] + \frac{\Gamma}{2} (\phi_i^{n+1} + \phi_i^n), \quad (7a)$$

$$i \frac{\phi_i^{n+1} - \phi_i^n}{\tau} = \frac{\beta}{2h^2} (\phi_{i-1}^{n+1} - 2\phi_i^{n+1} + \phi_{i+1}^{n+1} + \phi_{i-1}^n - 2\phi_i^n + \phi_{i+1}^n) \\ + \alpha_1 \frac{\phi_i^{n+1} + \phi_i^n}{4} \left[(|\phi_i^{n+1}|^2 + |\phi_i^n|^2) + (|\psi_i^{n+1}|^2 + |\psi_i^n|^2) \right] + \frac{\Gamma}{2} (\psi_i^{n+1} + \psi_i^n), \quad (7b)$$

on mesh (x_i, t^n) with $x_i = -L_1 + ih$, $h = (L_2 + L_1)/m$, $i = 1, \dots, m$ and $t^n = n\tau$, $n = 0, 1, 2, \dots$. It is not only convergent (consistent and stable), but also conserves mass and

energy, i.e., there exist discrete analogs M^n and E^n , for (2), which arise from the scheme (for details see [3, 7, 8]).

$$M^n = \sum_{i=2}^{N-1} (|\psi_i^n|^2 + |\phi_i^n|^2) = \text{const},$$

$$E^n = \sum_{i=2}^{N-1} \frac{-\beta}{2h^2} (|\psi_{i+1}^n - \psi_i^n|^2 + |\phi_{i+1}^n - \phi_i^n|^2) + \frac{\alpha_1}{4} (|\psi_i^n|^2 + |\phi_i^n|^2)^2 - \Gamma \Re[\bar{\phi}_i^n \psi_i^n] = \text{const},$$

for $n \geq 0$. These values are kept constant by the scheme during the time stepping. The above scheme is of Crank-Nicolson type for the linear terms and we employ internal iteration to achieve implicit approximation of the nonlinear terms, i.e., we use its linearized implementation [3]. In this way the order of approximation of Eqs. (7) is $O(\tau^2 + h^2)$. The detailed description of the method of internal iteration applied to CLNSEs can be found in [3].

The above presented scheme and algorithm have been verified for different grids and time increments and the approximation has been confirmed.

RESULTS AND DISCUSSION

We observe that the time oscillation (‘breathing’) of the amplitude of the soliton does not interfere with the soliton collision, i.e., the ‘breathing’ of the pulses take place even without any interaction. This distinguishes the solitons considered here from the breathers previously reported in the literature [11, 2]. One can say that the apparent breathing is actually a manifestation of the rotation of the polarization. In a sense, the linear coupling (parameterized by Γ) is responsible for the exchange of wave mass between the modes. Following [7] we call this effect ‘cross-dispersion’ of the signals. In Figures 1 and 2 we present these features for given Γ in both cases – head-on and takeover interaction.

Our observations show that the presented here interactions are independent of the initial phase difference $[[\delta]]$ and the trajectories of the centers of the QPs experience almost insignificant shift after the interaction. Thus, in the case of head-on collision given in Figure 1a, initial trajectories are given by $x = \pm 45 \mp t$ while the trajectories of the outgoing solitons are given by $x = \pm 44.7 \mp t$ (Figure 1b). The pseudomomentum varies between 10^{-15} (it vanishes due to the symmetry) in the beginning and 10^{-5} after the collision, i.e., it reasonable well approximates the trivial value. The small change is due to the reflection from the the boundary conditions at the finite boundaries of the computational interval. The energy and the total mass are conserved, $E = 0.2659$, $M = 2$ at each time moment but negligible oscillations of the energy after the fifth significant digit and of the component masses M_ψ and M_ϕ after the seventh significant digit are present. The parameter that undergoes the more significant evolution is the polarization angle. We begin with linear polarization ($\theta_l = 0^\circ$, $\theta_r = 90^\circ$) which evolves after the interaction (see Table 1, columns 2 and 3), but the sum is fairly well preserved (see Table

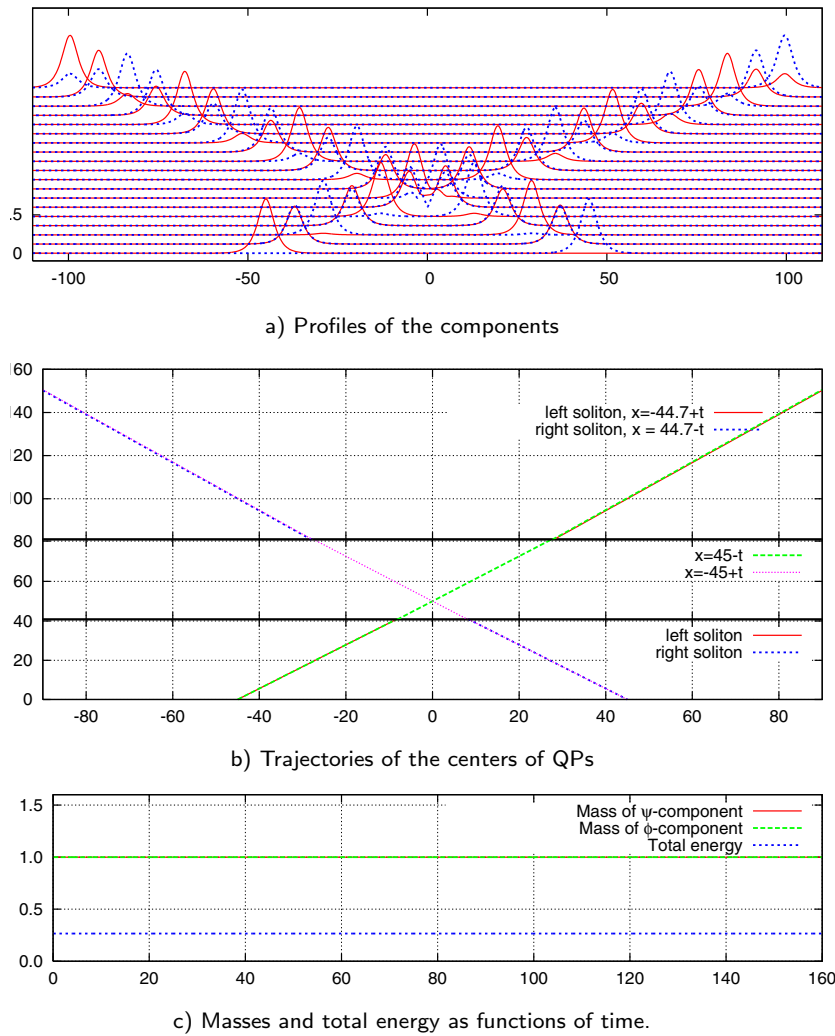


FIGURE 1. Head-on collision for $\Gamma = 0.1$. Linear initial polarization: $c_l = -c_r = 1$, $[\delta] = 90^\circ$.

1, column 4). The only place where the deviation of net polarization differs appreciably from 90° is at the moment of the interaction (see Table 1, row 3). The approximate

TABLE 1. “Breathing” dynamics of head-on interaction from Figure 1

t	θ_l	θ_r	$\theta_l + \theta_r$	M_ψ	M_ϕ	$M_\psi + M_\phi$	P	E
0	0°	90°	90°	1	1	2	0.1E-15	0.2659
8	$44^\circ 9'$	$45^\circ 50'$	$89^\circ 59'$	1	1	2	0.1E-13	0.2659
40	$48^\circ 33'$	$40^\circ 15'$	$88^\circ 48'$	0.99	1	1.99	-0.5745E-07	0.2659
120	$32^\circ 28'$	$57^\circ 31'$	$89^\circ 59'$	0.99	1	1.99	-0.2303E-04	0.2659
152	$29^\circ 08'$	$60^\circ 52'$	90°	0.99	1	1.99	-0.2294E-04	0.2659

conservation of the polarization has been found also in our previous works with essential

nonlinear coupling [9, 10].

The takeover interaction (Figure 2a) follows the same qualitative pattern but with a bigger phase shift of the slower soliton and smaller phase shift of the faster soliton (Figure 2b).

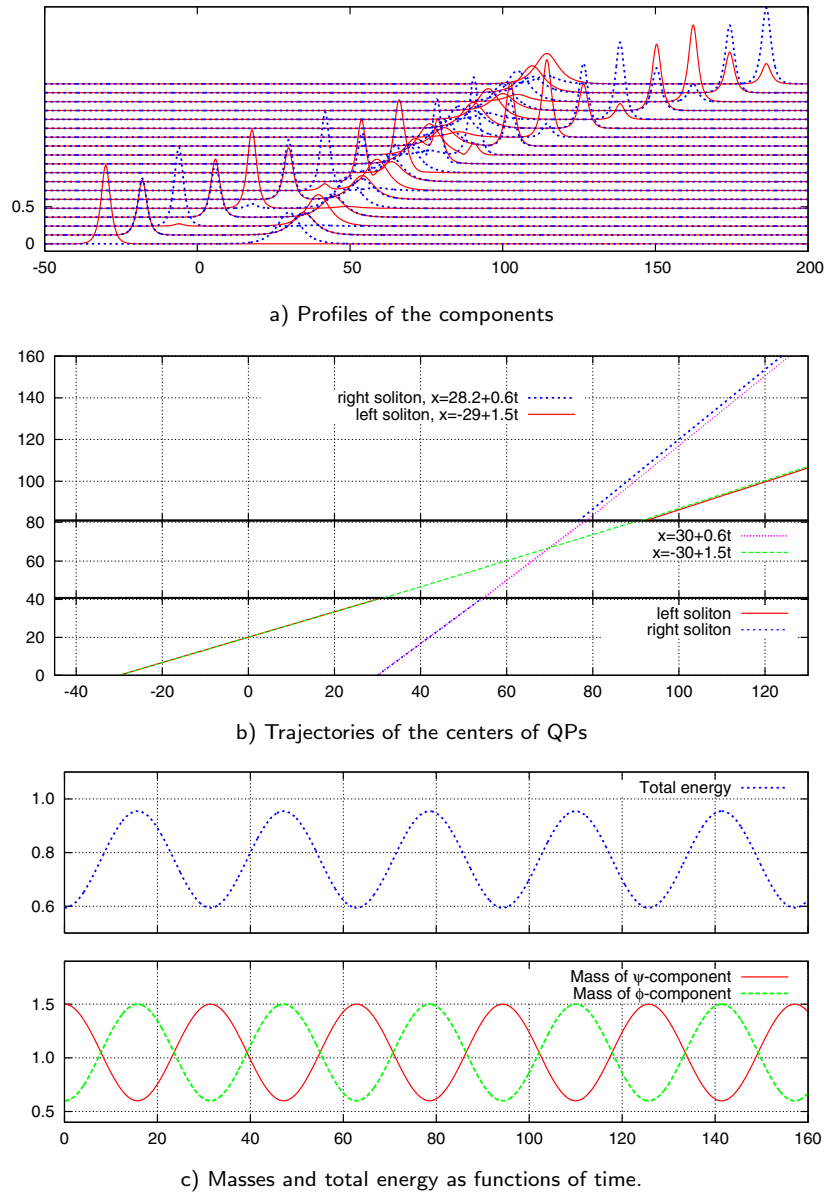


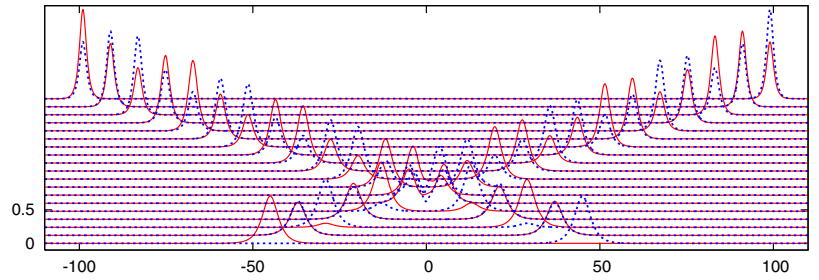
FIGURE 2. Takeover interaction for $\Gamma = 0.1$. Linear initial polarization: $c_l = 1.5$, $c_r = 0.6$, $[\delta] = 0^\circ$.

We note that the initial trajectories of centers shift from $x = -30 + 1.5t$ to $x = -29 + 1.5t$ and from $x = 30 + 0.6t$ to $x = 28.2 + 0.6t$ after the interaction. Compared to the previous case of head-on collision the interaction is longer and this is the reason for the larger phase shifts (see, e.g., [6] of the similar effect for KdV solitons). We

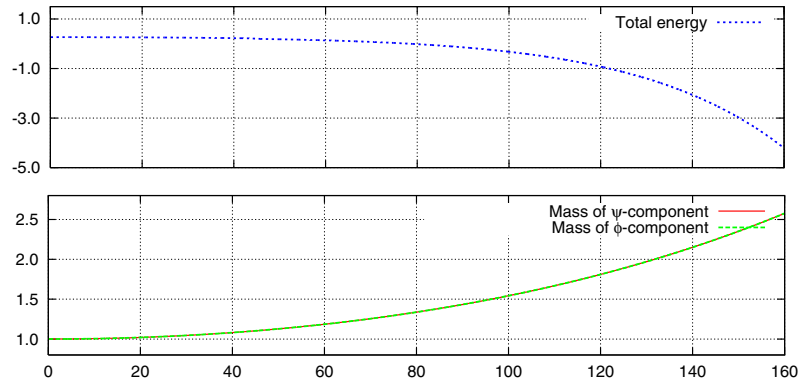
have found that the individual masses oscillate (breathe) by period determined by the magnitude of real part of the coupling parameter $\Re[\Gamma]$ (see Figure 2c), while the net mass is constant at $M = 2.1$ (see Table 2, column 7). Similarly, the total energy oscillates within the described period, but its magnitude is perfectly conserved within the full period (Figure 2c). The pseudomomentum is also conserved at $P = 2.6056$ (see Table 2, column 8). The notable feature here is that the rotational polarization originated by the linear coupling does not violate an excellent conservation of the total initial polarization $\theta_l + \theta_r = 90^\circ$ (see Table 2, column 4).

TABLE 2. ‘Breathing’ dynamics of takeover interaction from Figure 2

t	θ_l	θ_r	$\theta_l + \theta_r$	M_ψ	M_ϕ	$M_\psi + M_\phi$	P	E
0	0°	90°	90°	1.5	0.6	2.1	2.6056	0.5942378
8	$45^\circ 49'$	$44^\circ 10'$	$89^\circ 59'$	1.037	1.063	2.1	2.6056	0.7794071
72	$52^\circ 27'$	$37^\circ 29'$	$89^\circ 56'$	0.935	1.165	2.1	2.6056	0.8202960
120	$57^\circ 21'$	$32^\circ 36'$	$89^\circ 57'$	1.238	0.862	2.1	2.6056	0.6989592
152	$29^\circ 18'$	$60^\circ 43'$	$90^\circ 1'$	1.284	0.816	2.1	2.6056	0.6806916



a) Profiles of the components



b) Masses and total energy as functions of time.

FIGURE 3. Head-on interaction for $\Gamma = 0.1 + 0.005i$. Linear initial polarization: $c_l = -c_r = 1$, $[\delta] = 90^\circ$.

The above discussion is concerned with the *sech*-like initial conditions when the linear-coupling parameter is real. In order to complete our investigation we conduct series of experiments with initial conditions of kind (4a)-(4b) and complex-valued linear

TABLE 3. Complex (breathe+gain) dynamics of head-on interaction from Figure 3

t	θ_l	θ_r	$\theta_l + \theta_r$	P
0	0°	90°	90°	0.73305489E-16
40	40°45'	48°30'	89°15'	-0.63825632E-04
80	25°35'	64°25'	90°	-0.26786818E-04
120	51°41'	38°20'	90°01'	-0.17967968E-03
160	55°54'	34°05'	89°59'	-0.35057001E-03

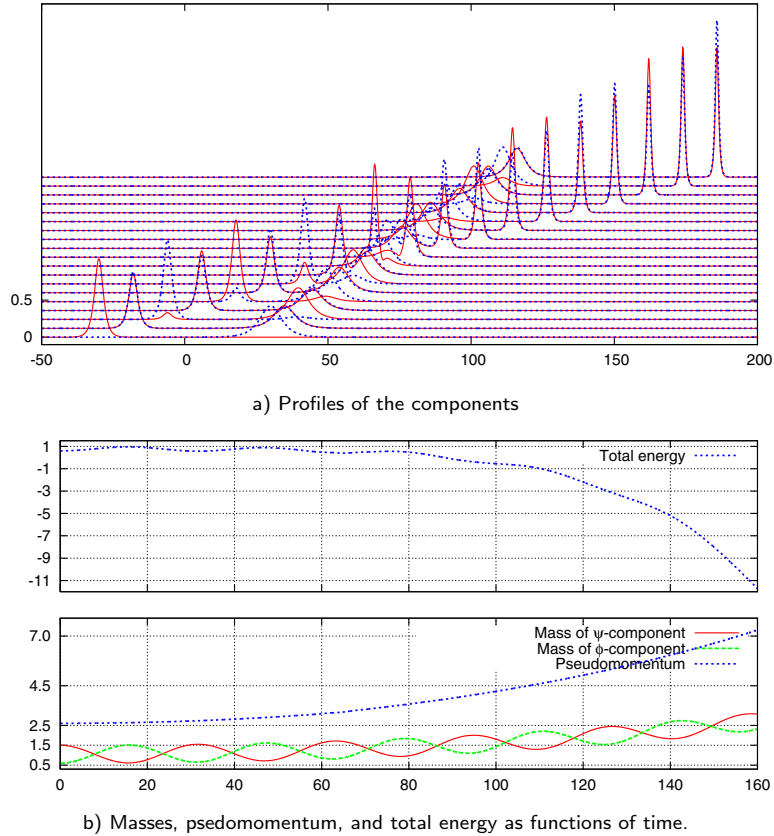


FIGURE 4. Takeover interaction for $\Gamma = 0.1 + 0.005i$. Linear initial polarization: $c_l = 1.5, c_r = 0.6$, $[\delta] = 90^\circ$.

coupling. For simplicity we use the same value for the real part, i.e., $\Gamma = 0.1 + 0.005i$. In Figure 3a we present the case of head-on collision for linear initial polarization. The nontrivial imaginary part of the linear coupling leads to violation of all observed conservation laws (Figure 3b): the masses increase exponentially while keeping equal to one another; the (negative) total energy decreases exponentially, too. The net pseudomomentum keeps its trivial value within good accuracy being in order of 10^{-17} in the beginning and 10^{-4} after the interaction (Table 3, column 5).

TABLE 4. Complex (breathe+gain) dynamics of takeover interaction from Figure 4

t	θ_l	θ_r	$\theta_l + \theta_r$	P
0	0°	90°	90°	2.6056
16	85°08'	4°52'	90°	2.6390
40	41°09'	48°49'	90°39'	2.8164
56	50°04'	40°48'	90°52'	3.0234
80	52°58'	54°14'	107°12'	3.5729
96	38°37'	36°45'	75°22'	4.0749
120	48°	8°43'	56°43'	5.0271
136	42°42'	77°38'	120°20'	5.8185
160	45°16'	40°13'	85°29'	7.2992

Concerning the magnitudes of the net polarization of each envelop we observed that they begin to breathe and gain amplitude right after the onset of time while keeping an excellent conservation of the total polarization before and after the interaction (see Table 3, column 4).

In the end we consider the case of takeover collision with complex parameter of linear coupling. Compared to the linear coupling with purely real coupling parameter (Figure 2) we again observe oscillations of the energy and masses (Figure 4b). The (negative) energy decreases very fast, while the masses M_ψ and M_ϕ increase all of them oscillating. The pseudomomentum P increases without appreciable oscillation. Table 4 presents the polarization. It is seen that the individual polarizations oscillate from the very beginning and the net total polarization is conserved only prior the interaction. After the interaction, the total polarization starts to oscillates, too (see Table 4, column 4). It is still an open question whether the polarization is conserved over on period of the oscillations.

CONCLUSION

In the present short note we solve numerically the vector NLSE with complex-valued linear coupling. We find that in the case of purely real linear coupling parameter, the energy, pseudomomentum, mass, and polarization are conserved over the period of oscillations (breathing), while adding an imaginary part to the parameter leads to violation of the conservation laws. Our computations confirm the well established fact for many different soliton systems that the phase shift depends on the duration of the interaction being larger for takeover collisions in comparison with the head-on collision.

REFERENCES

1. G. P. Agrawal, *Nonlinear Fiber Optics*, Academic, New York, 1989.
2. K. Chow, K. Nakkeeran, and B. Malomed, *Opt. Comm.* **219**, 251–259 (2003).
3. C. I. Christov, S. Dost, and G. A. Maugin, *Physica Scripta* **50**, 449–454 (1994).
4. C. I. Christov, “Gaussian elimination with pivoting for multidagonal systems,” *Internal Report* **4**, University of Reading, 1994.

5. H. A. Haus, and W. S. Wong, *Rev. Mod. Phys.* **68**, 423–444 (1996).
6. A. C. Newell, *Solitons in Mathematics and Physics*, SIAM, Philadelphia, 1985.
7. W. J. Sonnier, and C. I. Christov, *Math. Comp. Simul.* **69**, 514–525 (2005).
8. M. D. Todorov, and C. I. Christov, *Discrete and Continuous Dynamical Systems, Suppl. 2007*, 982–992.
9. M. D. Todorov, and C. I. Christov, *Discrete and Continuous Dynamical Systems, Suppl. 2009*, 780–789.
10. M. D. Todorov, and C. I. Christov, *Math. Comp. Simul.* **80**, 46–55 (2009).
11. H. Winful, *Appl. Phys. Lett.* **47**, 213–215 (1985).